Arabian Journal of Chemistry (2014) 7, 197–207

King Saud University

Arabian Journal of Chemistry

www.ksu.edu.sa
www.sciencedirect.com

ORIGINAL ARTICLE

Synthesis, characterization and corrosion inhibition efficiency of 2-(6-methylpyridin-2-yl)-1H-imidazo[4,5-f][1,10] phenanthroline on mild steel in sulphuric acid

N.O. Obi-Egbedi [a], I.B. Obot [b,*], A.O. Eseola [c]

[a] *Department of Chemistry, University of Ibadan, Ibadan, Nigeria*
[b] *Department of Chemistry, Faculty of Science, University of Uyo, P.M.B 1017, Uyo, Akwa Ibom State, Nigeria*
[c] *Chemical Sciences Department, Redeemer's University, Redemption City, Km. 46, Lagos – Ibadan Expressway, Nigeria*

Received 18 September 2010; accepted 24 October 2010
Available online 29 October 2010

KEYWORDS

Phenanthroline derivative;
Mild steel;
Corrosion inhibitors;
Sulphuric acid;
Thermodynamic

Abstract Phenanthroline derivative, 2-(6-methylpyridin-2-yl)-1H-imidazo[4,5-f][1,10] phenanthroline (MIP) was synthesized and characterized by elemental analysis, FT-IR, ^{1}H NMR, ^{13}C NMR, and single crystal X-ray diffraction study. MIP was evaluated as corrosion inhibitor for mild steel in 0.5 M H_2SO_4 solution using gravimetric and UV–Visible spectrophotometric methods at 303–333 K. Results obtained show that MIP acts as inhibitor for mild steel in H_2SO_4 solution. The inhibition efficiency was found to increase with increase in MIP concentration but decreased with temperature. Activation parameters and Gibbs free energy for the adsorption process using statistical physics were calculated and discussed. The UV–Visible absorption spectra of the solution containing the inhibitor after the immersion of mild steel specimen indicate the formation of a MIP-Fe complex.

© 2010 Production and hosting by Elsevier B.V. on behalf of King Saud University.

1. Introduction

The prevention of corrosion is vital not only for increasing the lifetime of equipments but also in decreasing the dissolution of toxic metals from the components into the environment (Solmaz, 2010). The use of organic molecules as corrosion inhibitors is one of the most practical methods for protecting metals against corrosion and it is becoming increasingly popular (Obi-Egbedi and Obot, 2012; Fouda et al., 2012). In recent years, a considerable amount of efforts is devoted to find novel, economical and efficient corrosion inhibitors of non-toxic type, which do not contain heavy metals and organic

* Corresponding author. Tel.: +234 8067476065.
E-mail address: proffoime@yahoo.com (I.B. Obot).
Peer review under responsibility of King Saud University.

ELSEVIER Production and hosting by Elsevier

1878-5352 © 2010 Production and hosting by Elsevier B.V. on behalf of King Saud University.
http://dx.doi.org/10.1016/j.arabjc.2010.10.025

phosphates. Inorganic compounds such as chromate, dichromate, nitrile and nitrate are widely used as corrosion inhibitors in several media and for different metals and alloys (Fontana, 1986). On the other hand, the biotoxicity of these products especially chromate is well documented (Hosseini and Azimi, 2009). Thus attention has now shifted to the use organic compounds bearing heteroatoms with high electron density for example phosphorus, sulphur, nitrogen, oxygen or those containing multiple bonds which are considered as adsorption centers as effective corrosion inhibitors (Obot and Obi-Egbedi, 2009, 2010; Ahamad and Quraishi, 2010; Abdallah and El-Naggar, 2001; Khaled et al., 2012).

Phenanthroline and its derivatives are an important class of compound present in many chemical structures of great interest in a variety of biochemical and industrial field. They form structural elements of important classes of pharmaceutical drugs such as antimalarial, antifungal, antitumoral, antiallergic, anti-inflammatory and antiviral drugs (Ignatushchenko et al., 2000; Gopalakrishnan et al., 1997; Pedraza-Chaverri et al., 2008). The choice of 2-(6-methylpyridin-2-yl)-1H-imidazo[4,5-f][1,10] phenanthroline (MIP) for the present investigation was based on the consideration: (i) it contains three heterocyclic moiety in one compound i.e. imidazole, pyridine and phenanthroline rings with several π-electrons and aromatic systems containing five *N* atoms, which can induce greater adsorption of the inhibitor molecule onto the surface of mild steel compared with compounds containing only one *N* atom like pyrrole already used as corrosion inhibitor; (ii) other considerations include: high electron-donating ability, the planarity of the molecular structure, electron density on the donor atoms, solubility and dispersibility. Moreover, the compound has a higher molecular weight (311.34 g mol^{-1}) than most *N*-heterocyclic compound already studied such as pyrrole and pyridine derivatives (Hudson et al., 1977; Bouklah et al., 2005). Furthermore, there is no report in the literature on the use of 2-(6-methylpyridin-2-yl)-1H-imidazo[4,5-f][1,10] phenanthroline as corrosion inhibitor for mild steel in sulphuric acid.

In continuation of our effort in developing corrosion inhibitors with high effectiveness and efficiency, the present paper explores the use of 2-(6-methylpyridin-2-yl)-1H-imidazo[4,5-f][1,10] phenanthroline as corrosion inhibitor for mild steel surface in sulphuric acid solution using gravimetric method and UV–Visible spectrophotometric methods. The effect of temperature is assessed in order to propose a suitable mechanism for the inhibitory action of MIP on the mild steel surface.

2. Experimental method

2.1. Synthesis of 2-(6-methylpyridin-2-yl)-1H-imidazo[4,5-f][1,10] phenanthroline

The inhibitor (MIP) was prepared with a procedure similar to that reported in the literature (Eseola et al., 2010). Phenanthroline-5,6-dione (3.00 g, 0.014 mol) and ammonium acetate (22 g, 0.29 mol) were weighed into the reaction flask and then charged with nitrogen atmosphere. Ethanol (15 mL), dichloromethane (15 mL), catalytic amount of glacial acetic acid (0.5 mL) and 6-methylpyridine-2-carboxaldehyde (2.18 g, 18.01 mmol, 1.25 equivalent) were added and the mixture was refluxed for 3 h. After cooling, the reaction mixture was neutralized by concentrated aqueous ammonia and the volume was reduced under reduced pressure. The organic components were extracted using dichloromethane (50 mL, thrice). The organic extracts were combined, concentrated and purified on silica gel column using ethyl acetate/petroleum ether (1:4) to elute the product. Portions containing the products were concentrated and addition of petroleum ether gave 2-(6-methylpyridin-2-yl)-1H-imidazo[4,5-f][1,10] phenanthroline as light yellow micro-crystals. X-ray was grown by slow diffusion of n-hexane into its dichloromethane solution. Fig. 1 shows the molecular structure of MIP.

2.1.1. Analytical data for inhibitor

Yield, 1.10 g, 24.5%. M.p. >300 °C. Selected IR peaks (KBr disc, cm^{-1}): *v* 3057s, 3016s, 1590m, 1562s, 1440s, 1068s, 739 vs. ^{1}H NMR (400 MHz, TMS, $CDCl_3$); δ 11.60 (br, s, 1H); 9.17 (d, J = 4.1 Hz, 2H); 9.05 (d, J = 8.2 Hz, 1H); 8.49 (d, J = 7.7 Hz, 1H); 8.52 (d, 7.6 Hz, 1H); 8.30 (d, J = 8.0 Hz, 1H); 7.80 (dd, J = 7.7 Hz, 1H); 7.74 (dd, J = 4.4, 8.0 Hz, 1H); 7.68 (dd, J = 4.4, 8.0 Hz, 1H); 7.24 (d, partially overlapped with $CDCl_3$ residual peak, 1H); 2,66 (s, 3H). Anal. Calc. For $C_{19}H_{13}N_5$: C, 72.25; H, 4.31; N, 22.17. Found: C, 72.47; H, 4.26; N, 22.05%.

2.2. Instrumentation

C, H and N analyses were carried out on a Flash EA 1112 micro-analyzer. ^{1}H NMR spectra were obtained with a Bruker ARX-400 MHz spectrometer using $CDCl_3$ as the solvent and TMS as an internal standard. Fourier transformation infrared (FT-IR) spectra were recorded in KBr pellets using Shimadzu 8740 FT-IR spectrometer as KBr discs in the range of 4000–400 cm^{-1}. The melting point was determined on a digital melting point instrument (Electrothermal model 9200). X-ray data were collected on Rigaku R-AXIS Rapid IP diffractometer (Rigaku Inc., 2008). The instrument employs graphite-monochromated Mo-Kα radiation operating at −100 °C. Cell parameters were obtained by global refinement of the positions of all collected reflections. Intensities were collected for Lorentz effects, polarization effects and empirical absorptions. The structure was solved by direct methods and refined by full-matrix least-squares on F^2. All non-hydrogen atoms were refined anisotropically and all hydrogen atoms were placed in calculated positions. Structure solution and refinement were performed using the SHELX-97 package (Esiola et al., 2010). Further details concerning X-ray data collection and refinement for 2-(6-methylpyridin-2-yl)-1H-imidazo[4,5-f][1,10] phenanthroline are given in Table 1.

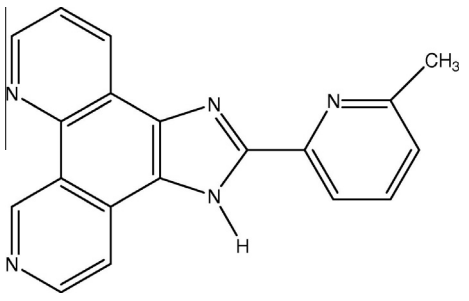

Figure 1 The molecular structure of 2-(6-methylpyridin-2-yl)-1H-imidazo[4,5-f][1,10] phenanthroline (MIP).

Table 1 Crystal data and structure refinement for 2-(6-methylpyridin-2-yl)-1H-imidazo[4,5-f][1,10] phenanthroline (MIP).

Empirical formula	$C_{19}H_{13}N_5$
Formula weight	311.34
Temperature (K)	173(2)
Wavelength (Å)	0.71073
Crystal system	Triclinic
Space group	$P\bar{1}$
Unit cell dimensions	a = 10.008(2) (Å) b = 12.402(3) (Å) c = 12.504(3) (Å) α = 88.88(3)° β = 78.17(3)°
Volume (Å^3)	1466.7(5)
Z	4
Density (calculated) (g m^{-3})	1.410
Absorption coefficient (mm^{-1})	0.089
F(0 0 0)	648
Crystal size (mm^3)	0.66 × 0.34 × 0.18
Theta range for data collection (°)	2.37–25.00
Index ranges	$-11 \le h \le 11$ $-14 \le k \le 14$ $-14 \le l \le 14$
Reflection collected	9390
Independent reflections	5143 [$R_{(int)}$ = 0.0650]
Completeness to theta = 25.00°	99.7%
Number of parameters	445
Goodness of fit on F^2	1.317
Final R indices [1 > 2sigma(I)]	R_1 = 0.0938, wR_2 = 0.1550
R indices (all data)	R_1 = 0.1266, wR_2 = 0.1657
Largest diff. peak and hole (e Å^{-3})	0.272 and −0.272

2.3. Material

Tests were performed on a freshly prepared sheet of mild steel of the following composition (wt.%): 0.13% C, 0.18% Si, 0.39% Mn, 0.40% P, 0.04% S, 0.025% Cu, and bal Fe. Specimens used in the weight loss experiment were mechanically cut into 5.0 cm × 4.0 cm × 0.8 cm dimensions, then abraded with SiC abrasive papers 320, 400 and 600 grit respectively, washed in absolute ethanol and acetone, dried in room temperature and stored in a moisture free dessicator before their use in corrosion studies (Obi-Egbedi and Obot, 2012).

2.4. Solutions

The aggressive solutions, 0.5 M H_2SO_4 were prepared by dilution of analytical grade 98% H_2SO_4 with distilled water. Stock solution of MIP was made in 10:1 water: methanol mixture to ensure solubility (Ahmad and Quraishi, 2010). This stock solution was used for all experimental purposes. The concentration range of MIP prepared and used in this study was 2 μM–10 μM.

2.5. Gravimetric measurements

The gravimetric method (weight loss) is probably the most widely used method of inhibition assessment (Musa et al., 2010; Khadom et al., 2010). The simplicity and reliability of the measurement offered by the weight loss method are such that the technique forms the baseline method of measurement in many corrosion monitoring programmes (Afidah and Kassim, 2008). Weight loss measurements were conducted under total immersion using 250 mL capacity beakers containing 200 mL test solution at 303–333 K maintained in a thermostated water bath. The mild steel coupons were weighed and suspended in the beaker with the help of rod and hook. The coupons were retrieved at 2 h interval progressively for 10 h, washed thoroughly in 20% NaOH solution containing 200 g/l of zinc dust (Obi-Egbedi and Obot, 2012) with bristle brush, rinsed severally in deionized water, cleaned, dried in acetone, and re-weighed. The weight loss, in grammes, was taken as the difference in the weight of the mild steel coupons before and after immersion in different test solutions. Then the tests were repeated at different temperatures. In order to get good reproducibility, experiments were carried out in triplicate. In this present study, the standard deviation values among parallel triplicate experiments were found to be smaller than 4%, indicating good reproducibility.

The corrosion rate (ρ) in mg cm^{-2} h^{-1} was calculated from the following equation (Umoren et al., 2010):

$$\rho = \frac{\Delta W}{St}, \tag{1}$$

where W is the average weight loss of three mild steel sheets, S is the total area of one mild steel specimen, and t is the immersion time (10 h). With the calculated corrosion rate, the inhibition efficiency (%I) was calculated as follows (Umoren et al., 2009a,b):

$$\%I = \left(\frac{\rho_1 - \rho_2}{\rho_1}\right) \times 100, \tag{2}$$

where ρ_1 and ρ_2 are the corrosion rates of the mild steel coupons in the absence and presence of inhibitor, respectively.

2.6. Spectrophotometric measurements

UV–Visible absorption spectrophotometric method was carried out on the prepared mild steel samples after immersion in 0.5 M H_2SO_4 with and without addition of 10 μM of MIP at 303 K for 3 days. All the spectral measurements were carried out using a Perkin–Elmer UV–Visible Lambda 2 spectrophotometer.

3. Results and discussion

3.1. Gravimetric studies

The electrochemical theory of corrosion proposed that corrosion of metals is largely accompanied by the action of a network of short-circuited electrolytic cells on the metal surfaces (Abiola et al., 2004). Iron (II) ions go into solution at the anodes of these cells in amount chemically equivalent to the reaction at the cathodes. The anodic dissolution reaction of iron in hydrochloric acid solution is as follows:

$$Fe \rightarrow Fe^{2+} + 2e. \tag{3}$$

On the other hand, the reaction at the cathodes which lead to hydrogen evolution can be represented as:

$$2H^+ + 2e \rightarrow 2H_{ads}, \tag{4}$$

$$2H_{ads} \rightarrow H_2. \tag{5}$$

Thus, Eqs. (3)–(5) lead to the corrosion of mild steel in sulphuric acid solution.

It is generally accepted that the first step in the adsorption of an organic inhibitor on a metal surface usually involves the displacement of one or more water molecules adsorbed at the metal surface (Umoren et al., 2008).

$$\mathrm{Inh}_{(sol)} + x\mathrm{H_2O} \leftrightarrow \mathrm{Inh}_{(ads)} + x\mathrm{H_2O}_{(sol)}, \quad (6)$$

where x is the size ratio, that is, the number of water molecules replaced by one organic inhibitor. The inhibitor may then combine with freshly generated Fe^{2+} ions on the steel surface (Eq. (3)), forming metal-inhibitor complexes:

$$Fe^{2+} + \mathrm{Inh}_{(ads)} \rightarrow [\mathrm{Fe\text{-}Inh}]^{2+}_{(ads)}. \quad (7)$$

The resulting complex could, depending on its relative solubility, either inhibit or catalyze further metal dissolution.

Weight loss measurements were carried out in a 0.5 M H_2SO_4 in the absence and presence of different concentrations of MIP at 303–333 K in order to determine the effectiveness of MIP as a corrosion inhibitor. Fig. 2 shows a representative plot of weight loss against time for mild steel in 0.5 M H_2SO_4 solution containing no inhibitor (blank) and in the presence of different concentrations of MIP at 303 K. The figure clearly shows a reduction in weight loss of the steel coupons in the presence of different concentrations of MIP compared to the free acid solution (blank). This shows that MIP actually inhibited the acid induced corrosion of mild steel in sulphuric acid. The non-uniformity and non-linearity of the curves of the weight loss plot may be attributed to the presence of mill scale on the mild steel surface. It may also suggest that the mild steel corrosion by H_2SO_4 is a heterogeneous process involving several steps. Similar observation has been reported recently (Solomon et al., 2010).

The average corrosion rates are shown in Table 2. The results show that MIP tested inhibits the corrosion of steel in 0.5 M H_2SO_4 solution. The corrosion rate was found to depend on the concentration of MIP and experimental temperature (Fig. 3). It is evident from Table 2 and Fig. 3 that the corrosion rate decreased with increasing inhibitor concentration but increased with rise in temperature.

Table 2 and Fig. 4 also show that inhibition efficiency (%I) increased with increasing inhibitor concentration and reached its maximum value of 72% at a concentration of 10 μM. The inhibitory behavior of MIP against mild steel corrosion can be attributed to the adsorption of MIP on the mild steel surface, which limits the dissolution of the latter by blocking of its corrosion sites and hence decreasing the corrosion rate with increasing efficiency as its concentration increases. The presence of imidazole and phenanthroline rings with several π-electrons and aromatic systems containing five N atoms in the structure of MIP can induce greater adsorption of the inhibitor molecule onto the surface of mild steel. This process is facilitated by the presence of vacant d-orbitals of low energy in iron as observed in transition metals. Recently, it was found that

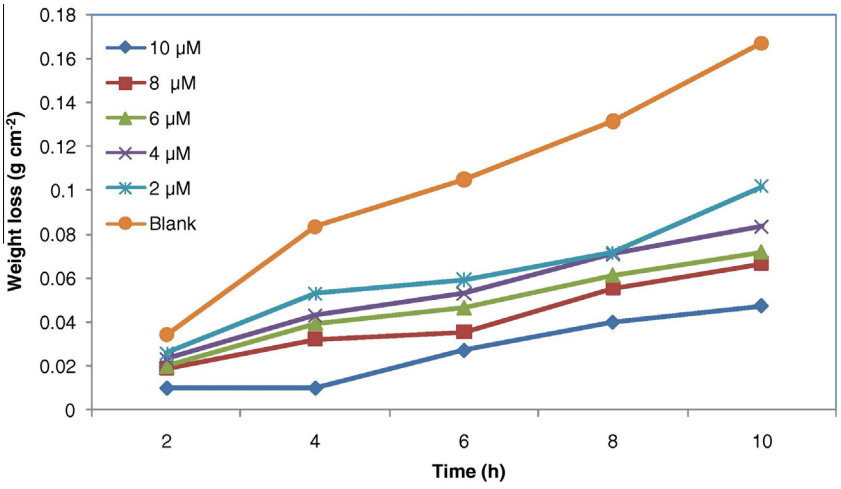

Figure 2 Variation of weight loss against time for mild steel corrosion in 0.5 M H_2SO_4 in the presence of different concentrations of MIP at 303 K.

Table 2 Calculated values of corrosion rate and inhibition efficiency for mild steel corrosion for mild steel in 0.5 M H_2SO_4 in the absence and presence of MIP at 303–333 K.

System/concentration (M)	Corrosion rate (mg cm^{-2} h^{-1})				Inhibition efficiency (%I)			
	303 (K)	313 (K)	323 (K)	333 (K)	303 (K)	313 (K)	323 (K)	333 (K)
Blank	0.83	1.91	4.46	6.14	–	–	–	–
2×10^{-6}	0.50	1.24	3.23	4.97	39	35	28	19
4×10^{-6}	0.42	1.07	3.01	4.61	50	44	33	25
6×10^{-6}	0.36	0.96	2.76	4.29	57	50	39	30
8×10^{-6}	0.35	0.79	2.47	3.81	60	59	45	38
10×10^{-6}	0.23	0.65	2.15	3.31	72	66	52	46

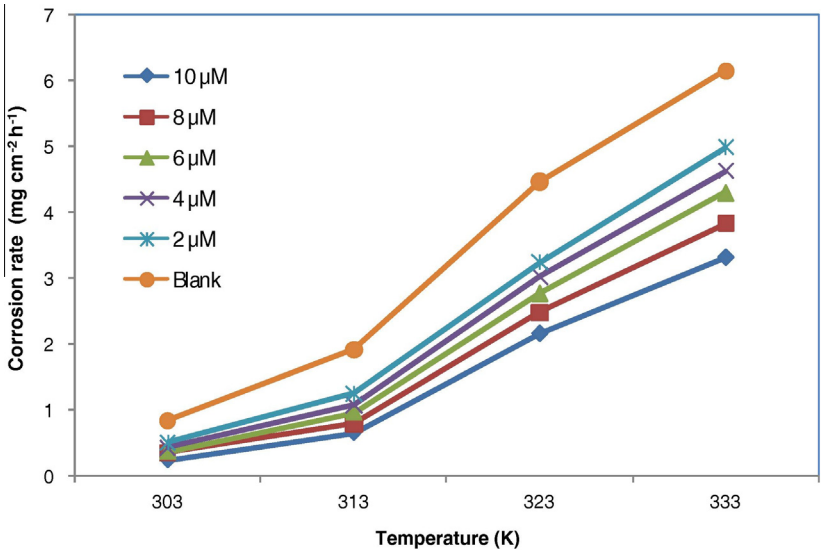

Figure 3 The relationship between corrosion rate and temperature for different concentrations of MIP.

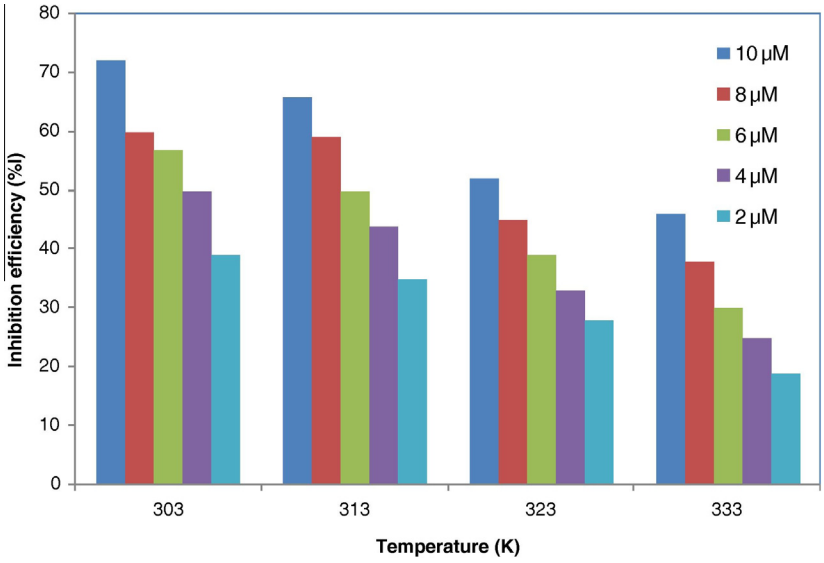

Figure 4 Variation of inhibition efficiency of MIP with temperature.

the formation of donor-acceptor surface complexes between free electrons of an inhibitor and a vacant d-orbital of a metal is responsible for the inhibition of the corrosion process (Khaled, 2010).

3.2. Effect of temperature

In acidic media, the corrosion of metal is generally accompanied with the evolution of H_2 gas. This is usually followed by an increase in temperature and the acceleration of the corrosion reaction which results in higher dissolution rate of the metal. Inspection of Table 2 shows that the corrosion rate increased with increasing temperature both in the uninhibited and inhibited solutions while the value of inhibition efficiency decreased with rise in temperature. A decrease in inhibition efficiency with increase in temperature may be due to the desorption of inhibitor molecules at higher temperatures. This has been attributed to physical adsorption of the inhibitor molecule on the mild steel surface (Obot and Obi-Egbedi, 2010).

It has been reported by a number of authors that for the acid corrosion of steel, the natural logarithm of the corrosion rate (ρ) is a linear function with $1/T$ (following the Arrhenius equation) (Soltani et al., 2010):

$$\log \rho = \log A - \frac{E_a}{2.303RT}, \tag{8}$$

where, ρ is the corrosion rate, E_a is the apparent activation energy, R is the molar gas constant (8.314 J K^{-1} mol^{-1}), T is the absolute temperature, and A is the frequency factor. The plot of log ρ against $1/T$ for mild steel corrosion in 0.5 M H_2SO_4 in

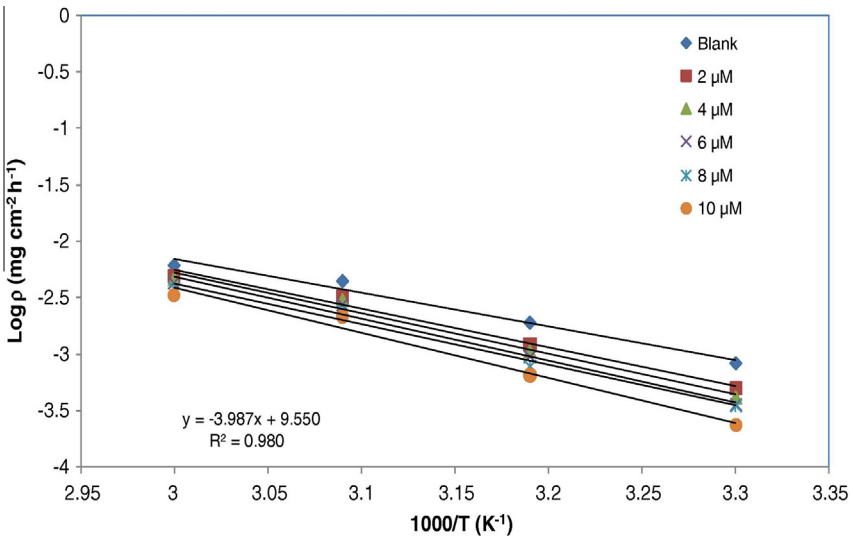

Figure 5 Arrhenius plot for mild steel corrosion in 0.5 M H_2SO_4 in the absence and presence of different concentrations of MIP.

the absence and presence of different concentrations of MIP is presented in Fig. 5. All parameters are given in Table 3.

Unchanged or lower values of E_a in inhibited systems compared to the blank have been reported (Morad and Kamal El-Dean, 2006) to be indicative of chemisorption mechanism, whereas higher values of E_a suggest a physical adsorption mechanism. According to the results obtained (Table 3), E_a values in the presence of MIP were higher than that in its absence (blank). The higher values of E_a in the inhibited solution can be correlated with the increased thickness of the double layer, which enhances the activation energy of the corrosion process (Behpour et al., 2009). The increase in activation energy after the addition of MIP to 0.5 M H_2SO_4 solution can indicate that physical adsorption (electrostatic interaction) occurs in the first stage. Indeed MIP molecule which contains several N atoms in its structure can be protonated to form cation forms in acid medium. It is logical to assume that in this case the electrostatic cation adsorption is responsible for the good protective properties of this compound. However, the adsorption phenomenon of an organic molecule is not considered only as a physical or as chemical adsorption phenomenon, but a wide spectrum of conditions, ranging from the dominance of chemisorption or electrostatic effects may arise due to the complex nature of the corrosion inhibiting process (Solmaz et al., 2008b).

Experimental corrosion rate values obtained from weight loss measurements for mild in 0.5 M H_2SO_4 in the absence and presence of MIP were used to further gain insight on the change of enthalpy (ΔH^*) and entropy (ΔS^*) of activation for the formation of the activation complex in the transition state using transition equation (Obot and Obi-Egbedi, 2010):

$$\rho = \left(\frac{RT}{Nh}\right) \exp\left(\frac{\Delta S^*}{R}\right) \exp\left(\frac{-\Delta H^*}{RT}\right), \tag{9}$$

where ρ is the corrosion rate, h is the Plank's constant (6.626176×10^{-34} J s), N is the Avogadro's number (6.02252×10^{23} mol^{-1}), R is the universal gas constant and T is the absolute temperature. Fig. 6 shows the plot of log ρ/T versus $1/T$ for mild steel corrosion in 0.5 M H_2SO_4 in the absence and presence of different concentrations of MIP. Straight lines were obtained with slope of ($\Delta H^*/2.303R$) and an intercept of [log (R/Nh) + ($\Delta S^*/2.303R$)] from which the values of ΔH^* and ΔS^* respectively were computed and listed also in Table 3. Inspection of these data reveals that the activation parameters (ΔH^* and ΔS^*) of dissolution reaction of mild steel in 0.5 M H_2SO_4 in the presence of MIP are higher than in the absence of inhibitor and also increase with increase in the concentration of MIP. The positive sign of the enthalpy of activation reflects the endothermic nature of steel dissolution process meaning that dissolution of steel is difficult (Guan et al., 2004). The entropy of activation was also positive in the absence and presence of MIP implying that the rate-determining step for the activated complex is dissociation step rather than association. In other words, the adsorption process is accompanied by an increase in entropy, which is the driving force for the adsorption of inhibitor onto the mild steel surface (Obi-Egbedi and Obot, 2010b).

Table 3 Activation parameters of the dissolution of mild steel in 0.5 M H_2SO_4 in the absence and presence of different concentrations of MIP.

C (M)	E_a (kJ mol^{-1})	ΔH^* (kJ mol^{-1})	ΔS^* (J mol^{-1} K^{-1})
Blank	57.21	230.14	369.95
2×10^{-6}	65.29	259.05	450.75
4×10^{-6}	68.73	270.35	483.31
6×10^{-6}	70.96	278.21	505.14
8×10^{-6}	74.94	282.25	521.45
10×10^{-6}	76.34	298.88	561.23

3.3. Thermodynamic consideration using the statistical model

Basic information on the interaction between inhibitor and mild steel surface can be provided by the thermodynamic parameters for the inhibiting process. The different types of adsorption expressions are determined by the different adsorption behavior of an organic inhibitor on mild steel surface. The inhibition process of an organic compound onto a metal surface can be explained by the formation of metal-inhibitor

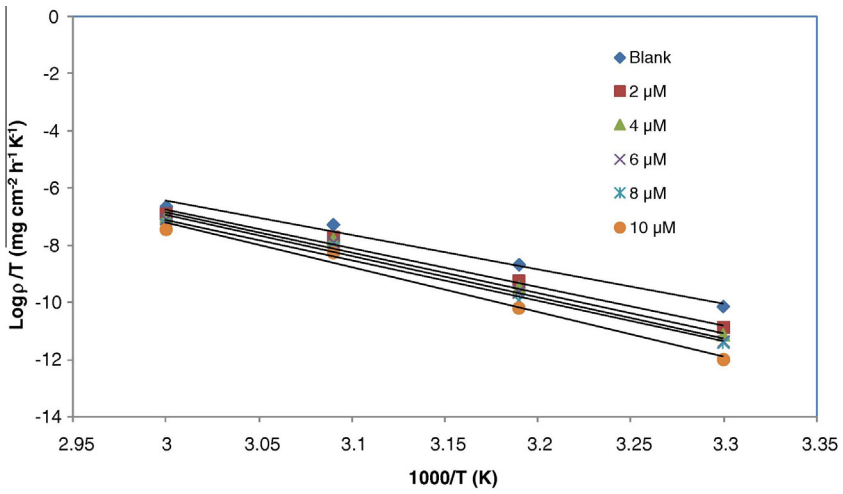

Figure 6 Transition state plot for mild steel corrosion in 0.5 M H_2SO_4 in the absence and presence of different concentrations of MIP.

reaction complex. The adsorption of an inhibitor species, I, on a metal surface, M, can be represented by a simplified equation:

$$M + I \leftrightarrow M(I)_{\text{ads}}. \tag{10}$$

Let M of the above reaction be the system in the ensemble and the solvent containing inhibitor molecules as donor particles be the medium. The complex-forming process can be regarded as the course of distribution of donor particles to the system. So it is justifiable to extend the model of variable number of particles in statistical physics for the inhibiting process.

According to statistical physics (Landau and Lifshitz, 1980), the probability of distribution for such kind of systems of variable number of particles is given by:

$$\varpi(i, \varepsilon) = A \exp\left(\frac{i\mu - \varepsilon_i}{\theta}\right), \tag{11}$$

where A is the normalizing coefficient, μ the chemical potential which depends upon the temperature and concentration of the donor particles, i the number of donor particles distributed in each system, θ the distribution modulus, ε_i is the energy of the system containing i donor particles, being assumed approximately equal for the systems containing the same number i of donor particles, and $\varepsilon_i = 0$ at $i = 0$.

The normalizing condition is:

$$\sum_{i=o}^{n} \varpi(i, \varepsilon) = 1 \tag{12}$$

or

$$\left\{1 + \sum_{i=1}^{n} \exp\left(\frac{i\mu - \varepsilon_i}{\theta}\right)\right\} = 1. \tag{13}$$

The average number of donor particles accepted by each system is:

$$\overline{n} = \sum_{i=1}^{n} i\varpi(i, \varepsilon) = \sum_{i=1}^{n} iA \exp\left(\frac{i\mu - \varepsilon_i}{\theta}\right) \tag{14}$$

Eliminating A from Eqs. (13) and (14), we obtain:

$$\overline{n} = \frac{\sum_{i=1}^{n} i \exp((i\mu - \varepsilon_i/)\theta)}{1 + \sum_{i=1}^{n} \exp((i\mu - \varepsilon_i/)\theta)}. \tag{15}$$

For inhibiting process, the $M(I)_{\text{ads}}$ formation reaction corresponds to the distribution with $i = 0$ or 1. The condition for which $i = 0$ is taken to correspond to a state of complete corrosion (surface coverage $\eta = 0$ and protection efficiency$\%I = 0$), $i = 1$ to a state of complete inhibition (surface coverage $\eta = 1$ and protection efficiency$\%I = 100$). The actual corrosion inhibition process is a random distribution between $i = 0$ and 1. So the corresponding actual protection efficiency ($\%I$) is a datum between 0 and 100, and the actual surface coverage η is equal to the statistical average value for such a (0, 1) distribution, then for inhibiting process, Eq. (15) is reduced to:

$$\overline{n} = \eta = \frac{1}{1 + \exp((\varepsilon - \mu)/\theta)}. \tag{16}$$

Here $0 < \overline{n} < 1$. Considering η is related to the concentration of donor particles and ε to the thermodynamic equilibrium constant of the complex-forming reaction, which is correlated to the change of free energy of adsorption ΔG^o_{ads}, thus the following equation can be derived from Eq. (16) (Wang et al., 2002; Obot and Obi-Egbedi, 2010):

$$\ln\left(\frac{1 - \eta}{\eta}\right) = \frac{\Delta G^o_{\text{ads}}}{\theta} - \frac{RT \ln C}{\theta}, \tag{17}$$

where C is the concentration of inhibitor particles.

The curve fitting of data in Table 2 to the statistical model at 303–333 K is presented in Fig. 7. Good correlation coefficient ($R^2 > 0.96$) was obtained. θ and ΔG^o_{ads} can be calculated from the slope and intercept of Eq. (15). All the calculated parameters are given in Table 4. The negative of ΔG^o_{ads} demonstrates that the inhibitor is spontaneously adsorbed onto the metal surface. Generally, the ΔG^o_{ads} values of -20 kJ mol^{-1} or less negative are consistent with physisorption, while those around -40 kJ mol^{-1} or more negative are associated with chemisorption as a result of the sharing or transfer of electrons from organic molecules to the metal surface to form a coordinate bond (Umoren et al., 2008). In the present study, the calculated values of ΔG^o_{ads} obtained for MIP ranges between -31.42 and -30.77 kJ mol^{-1} (Table 4), indicating that the adsorption of mechanism of MIP on mild steel in 0.5 M H_2SO_4 solution at the studied temperatures may be a

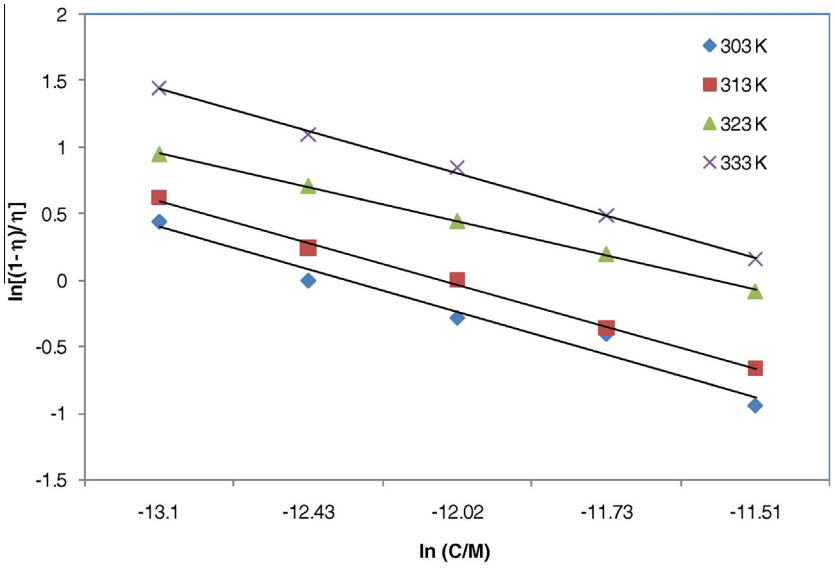

Figure 7 Application of the statistical model to the corrosion protection behavior of MIP.

combination of both physisorption and chemisorption (comprehensive adsorption) (Ahamad et al., 2010).

The enthalpy of adsorption can also be calculated from the Gibbs-Helmholtz equation (Singh and Quraishi, 2010):

$$\left[\frac{\partial(\Delta G^{o}_{ads}/T)}{\partial T}\right]_{p} = -\frac{\Delta H^{o}_{ads}}{T^{2}}. \quad (18)$$

Table 4 Some parameters from statistical model for mild steel in 0.5 M H_2SO_4 in the presence of MIP.

Temperature (K)	R^2	θ	ΔG^{o}_{ads} (kJ mol^{-1})
303	0.963	3.20×10^3	−31.42
313	0.996	3.30×10^3	−31.77
323	0.999	3.56×10^3	−30.81
333	0.997	4.30×10^3	−30.77

Eq. (18) can be arranged to give the following equation:

$$\frac{\Delta G^{o}_{ads}}{T} = \frac{\Delta H^{o}_{ads}}{T} + k. \quad (19)$$

The variation of $\Delta G^{o}_{ads}/T$ with 1/T gives a straight line with a slope which is equal to ΔH^{o}_{ads} (Fig. 8). It can be seen from the figure that $\Delta G^{o}_{ads}/T$ decreases with 1/T in a linear fashion. The obtained value of ΔH^{o}_{ads} was −22.00 kJ mol^{-1}.

The enthalpy and entropy for the adsorption of MIP on mild steel were also deduced from the thermodynamic basic equation (Abd El Rehim et al., 2010):

$$\Delta G^{o}_{ads} = \Delta H^{o}_{ads} - T\Delta S^{o}_{ads}, \quad (20)$$

where ΔH^{o}_{ads} and ΔS^{o}_{ads} are the enthalpy and entropy changes of adsorption process, respectively. A plot of ΔG^{o}_{ads} versus T was linear (Fig. 9) with the slope equal to $-\Delta S^{o}_{ads}$ and intercept of ΔH^{o}_{ads}. The enthalpy of adsorption ΔH^{o}_{ads}, and the entropy

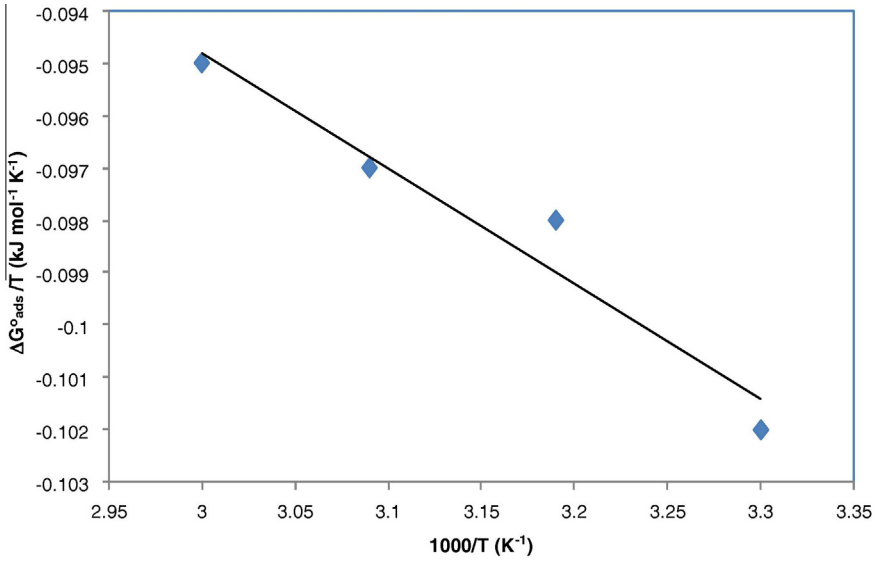

Figure 8 The variation of $\Delta G^{o}_{ads}/T$ with $1/T$.

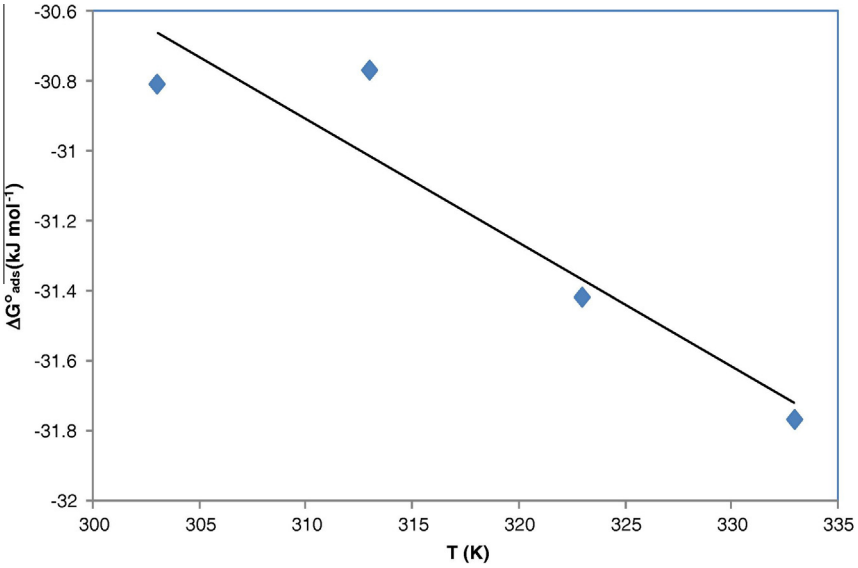

Figure 9 The variation of ΔG^{o}_{ads} with temperature.

of adsorption ΔS^{o}_{ads}, obtained are $-20.00\ kJ\ mol^{-1}$ and $35.00\ J\ mol^{-1}\ K^{-1}$ respectively. The enthalpy of adsorption ΔH^{o}_{ads} from the two approaches is in agreement. It has been reported that an endothermic adsorption process ($\Delta H^{o}_{ads} > 0$) is due to chemisorption while an exothermic adsorption process ($\Delta H^{o}_{ads} < 0$) may be attributed to physisorption, chemisorption or a mixture of both (Bentiss et al., 2005). When the process of adsorption is exothermic, physisorption can be distinguished from chemisorption according to the absolute value of ΔH^{o}_{ads}. For physisorption processes, this magnitude is usually lower than $40\ kJ\ mol^{-1}$ while that for chemisorption approaches $100\ kJ\ mol^{-1}$ (Bentiss et al., 1999). In this work, the negative sign of ΔH^{o}_{ads} is an indication that the adsorption of MIP on steel surface is exothermic while its absolute value suggests physisorption. However, the calculated values of ΔG^{o}_{ads} show that the adsorption of MIP is not merely physical or chemical but a combination of physisorption and chemisorption exists between the inhibitor and the metal surface (comprehensive adsorption) (Noor and Al-Moubaraki, 2008). The positive sign of ΔS^{o}_{ads} arises from substitutional process, which can be attributed to the increase in the solvent entropy and more positive water desorption entropy (Solmaz et al., 2008). This leads to an increase in disorder due to the fact that more water molecules can be desorbed from the metal surface by one inhibitor molecule (Avci, 2008).

3.4. UV–Visible spectroscopy

The adsorption of monochromatic light according to Abboud et al. (2007), is a suitable method for identification of complex ions. The adsorption of light is proportional to the concentration of the adsorbing species. For routine analysis, a simple conventional technique based on UV–Visible absorption is the most sensitive direct spectrophotometric detection. Change

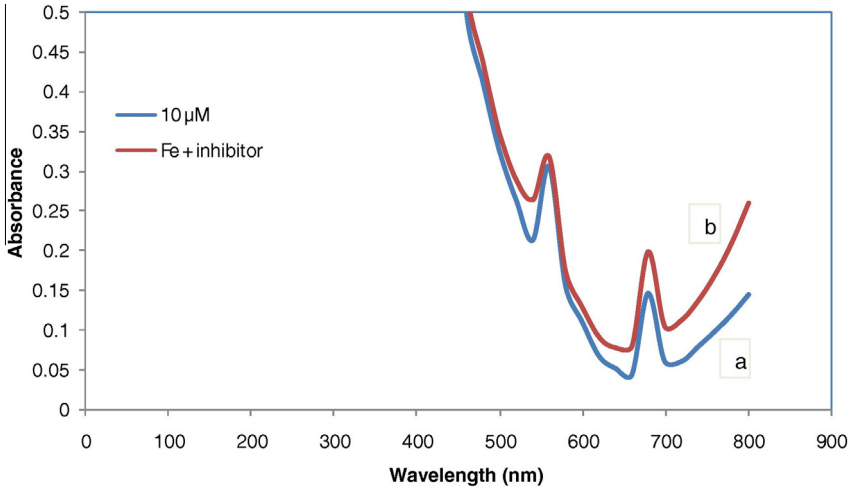

Figure 10 UV–Visible spectra of the solution containing 0.5 M H_2SO_4 (10 μM) MIP (a) before (blue) and (b) after 3 days of mild steel immersion (red).

in position of the absorbance maximum and change in the value of absorbance indicate the formation of a complex between two species in solution (Sherif and Park, 2005; Obi-Egbedi and Obot, 2010b).

In order to confirm the possibility of the formation of MIP-Fe complex, UV–Visible absorption spectra obtained from 0.5 M H_2SO_4 solution containing 10 μM MIP before and after 3 days of mild steel immersion is shown in Fig. 10. The electronic absorption spectra of MIP before the steel immersion display two bands in the visible region (550 and 680 nm). The absorption bands at this longer wavelengths are as a result of the presence of aromatic systems in MIP which are highly conjugated. These bands may also be assigned to π–π* transition involving the whole electronic structure system of the compound with a considerable charge transfer character (Aboud et al., 2009). After 3 days of steel immersion (Fig. 10), it is evident that there is an increase in the absorbance of this band. However, there was no significant difference in the shape of the spectra before and after the immersion of MIP showing a possibility of weak interaction between MIP and mild steel (physisorption). These experimental findings give strong evidence for the possibility of the formation of a complex between Fe^{2+} cation and MIP in H_2SO_4.

3.5. Mechanism of inhibition action of MIP on mild steel

From the experimental and theoretical results obtained, we note that a plausible mechanism of corrosion inhibition of mild steel in 0.5 M H_2SO_4 by MIP may be deduced on the basis of adsorption. In acidic solutions the inhibitor can exist as cationic species (Eq. (21)) which may be adsorbed on the cathodic sites of the mild steel and reduce the evolution of hydrogen:

$$MIP + 2H^+ \leftrightarrow [MIPH]^{2+}. \quad (21)$$

The protonated MIP, however, could be attached to the mild steel surface by means of electrostatic interaction between SO_4^{2-} and protonated MIP since the steel surface has positive charges in the acid medium (Li et al., 2005). This could futher be explained based on the assumption that in the presence of SO_4^{2-}, the negatively charged SO_4^{2-} would attach to positively charged surface. When MIP adsorbs on the steel surface, electrostatic interaction takes place by partial transference of electrons from the polar atoms (*N* atoms and the delocalized π electrons around the heterocyclic rings) of MIP to the metal surface. In addition to electrostatic interaction (physisorption) of MIP molecules on the steel surface, molecular adsorption may also play a role in the adsorption process. Similar mechanism has been proposed by us recently (Obi-Egbedi and Obot, 2010b).

4. Conclusions

The following conclusions may be drawn from the study:

1. 2-(6-methylpyridin-2-yl)-1H-imidazo[4,5-f][1,10] phenanthroline (MIP) acts as an inhibitor for the corrosion of mild steel in 0.5 M H_2SO_4. Inhibition efficiency values increase with the inhibitor concentration but decrease with temperature. The trend of inhibition efficiency with temperature and the increase in the activation energy in the presence of MIP suggest physical adsorption mechanism although chemisorption may also play a part in the inhibiting process.
2. The Gibbs free energy for the adsorption process calculated using statistical physics is negative indicating that the process is spontaneous.
3. UV–Visible spectrophotometric studies clearly reveal the formation of Fe–MIP complex which may be responsible for the observed inhibition.
4. This present study provides new information on the inhibiting characteristics of MIP under specified conditions. The new inhibitor could find possible applications in metal surface anodizing and surface coating in industries.

Acknowledgements

The authors wish to acknowledge the Department of Chemistry, University of Uyo, Nigeria, for providing the facilities for the work. One of the authors Dr. A.O. Eseola is also acknowledged for providing the newly synthesized inhibitor used in this research.

References

Abboud, Y., Abourriche, A., Saffaj, T., Berrada, M., Charrouf, M., Bennamara, A., Al-Himidi, N., Hannache, H., 2007. Mater. Chem. Phys. 105, 1.
Abboud, Y., Abourriche, A., Saffaj, T., Berrada, M., Charrouf, M., Bennamara, A., Hannache, H., 2009. Desalination 237, 175.
Abd El Rehim, S.S., Sayyah, S.M., El-Deeb, M.M., Kamal, S.M., Azooz, R.E., xxxx. Mater. Chem. Phys. 123, 20.
Abdallah, M., El-Naggar, M.M., 2001. Mater. Chem. Phys. 71, 291.
Abiola, O.K., Oforka, N.C., Argaye, S.S., 2004. Mater. Lett. 58, 3461.
Afidah, A.R., Kassim, J., 2008. Recent Patents Mater. Sci. 1, 223.
Ahamad, I., Prasad, R., Quraishi, M.A., 2010. Corros. Sci. 52, 1472.
Ahamad, I., Quraishi, M.A., 2010. Corros. Sci. 52, 651.
Avci, G., 2008. Colloid Surf. A: Physicochem. Eng. Asp. 317, 730.
Behpour, M., Ghoreishi, S.M., Gandomi-Niasar, A., Soltani, N., Salavati-Niasari, M., 2009. J. Mater. Sci. 44, 2444.
Bentiss, F., Lagrenee, M., Traisnel, M., Hornez, J.C., 1999. Corros. Sci. 41, 789.
Bentiss, F., Lebrini, M., Lagrenee, M., 2005. Corros. Sci. 47, 2915.
Bouklah, M., Quassini, A., Hammouti, B., El Idrissi, A., 2005. Appl. Surf. Sci. 250, 50.
Eseola, A.O., Zhang, M., Xiang, J.F., Zou, W., Li, Y., Woods, J.A.O., Sun, W.H., 2010. Inorg. Chim. Acta. http://dx.doi.org/10.1016/j.ica.2009.02.026.
Fontana, M.G., 1986. Corrosion Engineering, third ed. McGraw-Hill, Singapore.
Fouda, A.S., Abdallah, M., Ahmed, I.S., Eissa, M., 2012. Arab. J. Chem. 5, 297.
Gopalakrishnan, G., Banumathi, B., Suresh, G., 1997. J. Nat. Prod. 60 (5), 519.
Guan, N.M., Xueming, I., Fei, I., 2004. Mater. Chem. Phys. 86, 59.
Hosseini, S.M.A., Azimi, A., 2009. Corros. Sci. 51, 728.
Hudson, R.M., Bulter, T.J., Warning, C.J., 1977. Corros. Sci. 17, 571.
Ignatushchenko, M.V., Winter, R.W., Riscoe, M., 2000. Am. J. Trop. Med. Hgy. 62 (1), 77.
Khadom, A.A., Yaro, A.S., Kadum, A.H., 2010. J. Taiwan Ins. Chem. Eng. 41, 122.
Khaled, K.F., Abdel-Rehim, S.S., Saker, G.B., 2012. Arab. J. Chem. 5, 213.
Khaled, K.F., 2010. Corros. Sci.. http://dx.doi.org/10.1016/j.corsci.2010.05.039.

Landau, L.D., Lifshitz, E.M., 1980. Statistical Physics. Pergamon Press, Oxford, p. 107.
Li, Y., Zhao, P., Liang, Q., Hou, B., 2005. Appl. Surf. Sci. 252, 1245.
Morad, M.S., Kamal El-Dean, A.M., 2006. Corros. Sci. 50, 55.
Musa, A.Y., Khadom, A.A., Kadhum, A., Mohamad, H., Takriff, M.S., 2010. J. Taiwan Ins. Chem. Eng. 41, 126.
Noor, E.A., Al-Moubaraki, A.H., 2008. Mater. Chem. Phys. 110, 145.
Obi-Egbedi, N.O., Obot, I.B., 2012. Arab. J. Chem. 5, 121.
Obi-Egbedi, N.O., Obot, I.B., 2010b. Corros. Sci.. http://dx.doi.org/10.1016/j.corsci.2010.09.020.
Obot, I.B., Obi-Egbedi, N.O., 2009. Corros. Sci. 52, 276.
Obot, I.B., Obi-Egbedi, N.O., 2010. Curr. Appl. Phys.. http://dx.doi.org/10.1016/j.cap. 2010.08.007.
Pedraza-Chaverri, J., Cardenas-Rodriguez, N., Orozco-Ibarra, M., Perez-Rojas, J.M., 2008. Food. Chem. Toxicol. 46 (10), 3227.
Sherif, E.M., Park, S.M., 2005. J. Electrochem. Soc. 152, B428.
Singh, A.K., Quraishi, M.A., 2010. Corros. Sci. 52, 152.
Solmaz, R., 2010. Corros. Sci.. http://dx.doi.org/10.1016/j.corsci.2010.06.001.
Solmaz, R., Kardas, G., Culha, M., Yazici, B., Erbil, M., 2008a. Electrochim. Acta 53, 5941.
Solmaz, R., Kardas, G., Yazici, B., Erbil, M., 2008b. Colloids Surf. A: Physicochem. Eng. Asp. 312, 7.
Solomon, M.M., Umoren, S.A., Udosoro, I.I., Udoh, A.P., 2010. Corros. Sci. 52 (4) 1317.
Soltani, N., Behpour, M., Ghoreishi, S.M., Naeimi, H., 2010. Corros. Sci. 52, 1351.
Umoren, S.A., Obot, I.B., Obi-Egbedi, N.O., 2009a. J. Mater. Sci. 44, 274.
Umoren, S.A., Obot, I.B., Ebenso, E.E., Obi-Egbedi, N.O., 2008. Int. J. Electrochem. Sci. 3, 1029.
Umoren, S.A., Obot, I.B., Ebenso, E.E., Obi-Egbedi, N.O., 2009a. Desalination. 247, 561.
Umoren, S.A., Solomon, M.M., Udousoro, I.I., Udoh A.P., 2010. Cellulose. 17, 635.
Wang, H.L., Fan, H.B., Zheng, J.S., 2002. Mater. Chem. Phys. 77, 655.